

University of Groningen

Giant tunnel electroresistance with PbTiO₃ ferroelectric tunnel barriers

Crassous, A.; Garcia, V.; Bouzehouane, K.; Fusil, S.; Vlooswijk, A. H. G.; Rispens, G.; Noheda, B.; Bibes, M.; Barthelemy, A.

Published in:
Applied Physics Letters

DOI:
[10.1063/1.3295700](https://doi.org/10.1063/1.3295700)

IMPORTANT NOTE: You are advised to consult the publisher's version (publisher's PDF) if you wish to cite from it. Please check the document version below.

Document Version
Publisher's PDF, also known as Version of record

Publication date:
2010

[Link to publication in University of Groningen/UMCG research database](#)

Citation for published version (APA):

Crassous, A., Garcia, V., Bouzehouane, K., Fusil, S., Vlooswijk, A. H. G., Rispens, G., Noheda, B., Bibes, M., & Barthelemy, A. (2010). Giant tunnel electroresistance with PbTiO₃ ferroelectric tunnel barriers. *Applied Physics Letters*, 96(4), 042901-1-042901-3. [042901]. <https://doi.org/10.1063/1.3295700>

Copyright

Other than for strictly personal use, it is not permitted to download or to forward/distribute the text or part of it without the consent of the author(s) and/or copyright holder(s), unless the work is under an open content license (like Creative Commons).

The publication may also be distributed here under the terms of Article 25fa of the Dutch Copyright Act, indicated by the "Taverne" license. More information can be found on the University of Groningen website: <https://www.rug.nl/library/open-access/self-archiving-pure/taverne-amendment>.

Take-down policy

If you believe that this document breaches copyright please contact us providing details, and we will remove access to the work immediately and investigate your claim.

Downloaded from the University of Groningen/UMCG research database (Pure): <http://www.rug.nl/research/portal>. For technical reasons the number of authors shown on this cover page is limited to 10 maximum.

Giant tunnel electroresistance with PbTiO₃ ferroelectric tunnel barriers

A. Crassous,¹ V. Garcia,¹ K. Bouzehouane,¹ S. Fusil,^{1,2} A. H. G. Vlooswijk,³ G. Rispens,³ B. Noheda,³ M. Bibes,^{1,a)} and A. Barthélemy¹

¹Unité Mixte de Physique CNRS/Thales, 1 Av. A. Fresnel, Campus de l'Ecole Polytechnique, 91767 Palaiseau, France and Université Paris-Sud, 91405 Orsay, France

²Université d'Evry-Val d'Essonne, Bd. F. Mitterrand, 91025 Evry Cedex, France

³Zernike Institute for Advanced Materials, University of Groningen, Groningen 9747AG, The Netherlands

(Received 16 November 2009; accepted 29 December 2009; published online 25 January 2010)

The persistency of ferroelectricity in ultrathin films allows their use as tunnel barriers. Ferroelectric tunnel junctions are used to explore the tunneling electroresistance effect—a change in the electrical resistance associated with polarization reversal in the ferroelectric barrier layer—resulting from the interplay between ferroelectricity and quantum-mechanical tunneling. Here, we use piezoresponse force microscopy and conductive-tip atomic force microscopy at room temperature to demonstrate the resistive readout of the polarization state through its influence on the tunnel current in PbTiO₃ ultrathin ferroelectric films. The tunnel electroresistance reaches values of 50 000% through a 3.6 nm PbTiO₃ film. © 2010 American Institute of Physics. [doi:10.1063/1.3295700]

Ferroelectrics are intensively studied for their applications in electronic devices such as nonvolatile ferroelectric random-access memories.¹ These devices are mainly based on ~100 nm thick ferroelectrics. At these thicknesses, various mechanisms of leakage currents were identified as Poole–Frenkel emission, space charge, Fowler–Nordheim tunneling, and Schottky emission.² When the thickness of the ferroelectric films decreases down to a few nanometer, direct mechanical quantum tunneling becomes the dominant leakage mechanism. In 1971, Esaki *et al.*³ originally proposed that switching the polarization of a ferroelectric tunnel barrier could lead to changes of the tunnel current. Nevertheless, as ferroelectricity is a cooperative phenomenon, it is usually accepted that there exists a fundamental thickness below which ferroelectricity collapses. For a long time, this critical thickness was believed to be well above a few nanometer and ferroelectric tunnel junctions were considered as purely conceptual. Due to tremendous technological advances in the growth of oxide thin films over the last decade, ferroelectric thin films of a few unit-cells are now achievable. This critical thickness (t_c) was determined for common ferroelectric materials such as the perovskite BaTiO₃ (BTO), PbTiO₃ (PTO), and BiFeO₃ (BFO) using x-ray photoemission diffraction,⁴ x-ray scattering,⁵ and piezoresponse force microscopy (PFM).⁶ Besides the nature of the ferroelectric material, t_c also depends on several factors, such as the electrode materials (through their ability to efficiently screen polarization charges), the strain state, or the ambient atmosphere giving rise to partial or complete screening on the ferroelectric surface. Experimentally, the lowest reported t_c values are 1 nm for BTO (Ref. 7), 1.2 nm for PTO (Ref. 5), and 2 nm for BFO (Ref. 6).

In 2003, the observation of resistive switching from Contreras *et al.*⁸ through 6 nm thick (Pb,Zr)/TiO₃ (PZT) tunnel barriers triggered a renewed interest for ferroelectric tunnel junctions. Tsymbal and Kohlstedt⁹ recently reviewed several possible mechanisms that can lead to resistance

variations in ferroelectric tunnel junctions (FTJs). In a classical tunnel junction, the current is an exponential function of the barrier height and thickness, and also depends on the density of states at the barrier/electrode interfaces. In FTJs, electrostatic effects may modify the barrier height,^{10,11} converse piezoelectric effects may modify the barrier thickness¹⁰ during the resistive readout of the polarization and the interfacial density of states may change depending on the polarization direction.⁹ The tunnel current is thus modified according to the polarization state of the ferroelectric ultrathin film, giving rise to a tunnel electroresistance (TER) phenomenon.¹² Recently, Garcia *et al.*⁷ and Gruverman *et al.*¹³ reported giant TER experiments through BTO tunnel barriers at room-temperature. In this letter, we focus on ultrathin PTO films used as tunnel barriers in ferroelectric tunnel junctions displaying a giant TER effect.

PbTiO₃/SrRuO₃ bilayers were deposited by pulsed laser deposition on (001) oriented SrTiO₃ substrates. Prior to deposition, the substrates were treated as described by Koster *et al.*¹⁴ to ensure a preferentially TiO₂-terminated terraced surface. The growth was monitored *in situ* by reflection high-energy electron diffraction (RHEED), which allows the thickness to be controlled at the unit cell level, see Figs. 1(a) and 1(b). The operation voltage of the differentially pumped RHEED (Ref. 15) was 28 kV and the filament current varied between 1.2 and 1.3 A. 45 nm thick SRO electrodes were grown using a 2.5 J/cm² ablation energy density while maintaining 0.06 mbar of O₂ in the deposition chamber and a substrate temperature of 700 °C. Four and nine unit cells thick (1.6 and 3.6 nm) PTO films (PTO_{4ML} and PTO_{9ML}, respectively) were grown using a 2 J/cm² energy density in 0.13 mbar of O₂ and a substrate temperature of 570 °C. The PTO was grown immediately after the SRO without removing the sample from the chamber and the samples were annealed only after the PTO deposition in 200 mbar of O₂ during a 5 °C/min cool down. A low root-mean-square surface roughness of 0.51 and 0.33 nm was determined using an atomic force microscope (AFM) in tapping mode for PTO_{4ML} and PTO_{9ML}, respectively [Figs. 1(c) and 1(d)]. Atomic steps are visible on the PTO_{4ML} film.

^{a)}Author to whom correspondence should be addressed. Electronic mail: manuel.bibes@thalesgroup.com.

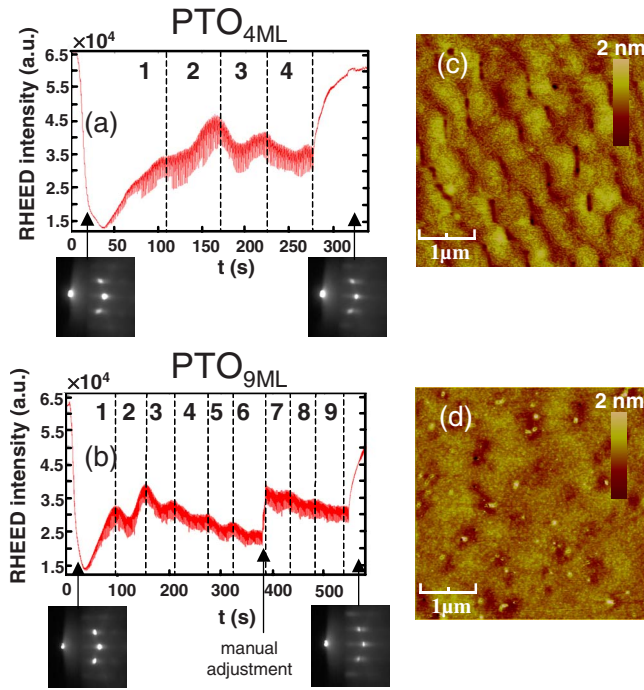


FIG. 1. (Color online) RHEED oscillations and diffraction patterns for (a) PTO_{4ML} and (b) PTO_{9ML}. Surface morphology of the (c) 4ML and (d) 9ML thin films characterized by tapping mode AFM over $5 \times 5 \mu\text{m}^2$ images.

An AFM operated in the so-called piezoresponse mode (multimode, nanoscope IV controller from Veeco and external SR830 lock-in amplifier from Stanford Research) was used to characterize the ferroelectric properties of the samples at room temperature, in a nitrogen flow. The determination of the polarization state of the PTO was performed with CrPt tips at an ac excitation frequency of 4 kHz and a voltage of 1 V. Figures 2(b) and 2(e) shows out-of-plane piezoresponse phase (OPP) images after poling with a negative and positive tip-SRO voltage along $4 \times 8 \mu\text{m}^2$ stripes

the PTO_{4ML} and PTO_{9ML} films. Bias voltages of ± 4 V dc were applied to the PTO_{4ML} and PTO_{9ML} (the ground is connected to the SRO electrode) in order to pattern two distinct regions of opposite polarization. These bias voltages correspond to electric fields of 25 and 11 MV/cm, respectively. The high electric field values required to pole PTO ultrathin films are consistent with those determined previously using PFM for PTO and BTO films.^{16,7} 43 and 35 MV/cm were required to pole a 2.8 nm PTO film and a 1 nm BTO film, respectively. A large OPP contrast ($\sim 180^\circ$) is observed indicating that domains with opposite polarizations were indeed written in the PTO_{9ML} film. An OPP contrast of $\sim 110^\circ$ is obtained with the PTO_{4ML} film. Possible electrostatic effects could be superimposed to the lower amplitude PFM signal of the 4ML films and induce a reduction of the OPP contrast.¹⁷ We verified that poling and scanning do not affect the surface topography, as shown in Figs. 2(a) and 2(d).

To determine the influence of the polarization state of the ferroelectric on the tunnel current, we use a conductive tip atomic force microscope (CTAFM) with a 10^{-12} – 10^{-4} A current range and Si tips coated with B-doped diamond. $12 \times 12 \mu\text{m}^2$ resistance maps over the previously poled domains were collected at a tip-SRO bias voltage of 2 V. The resistance difference measured with the CTAFM between positively and negatively poled regions corresponds to the TER effect. Figures 2(c) and 2(f) displays the resistance difference between positively and negatively poled regions in the PTO_{4ML} and PTO_{9ML} films. The TER effect reaches about 4,000% in the PTO_{4ML} film and increases up to 50 000% in the PTO_{9ML} film. This increase may be explained by the exponential dependence of the TER with the film thickness, as predicted by electrostatic models¹¹ and reported on BTO ultrathin films.⁷ In addition, the lower resistance state corresponds to the ferroelectric polarization of PTO pointing toward SRO. Similarly, the tunnel resistance is lower in BTO/La_{0.67}Sr_{0.33}MnO₃ (LSMO) bilayers when the polarization points toward LSMO.⁷ This may indicate that

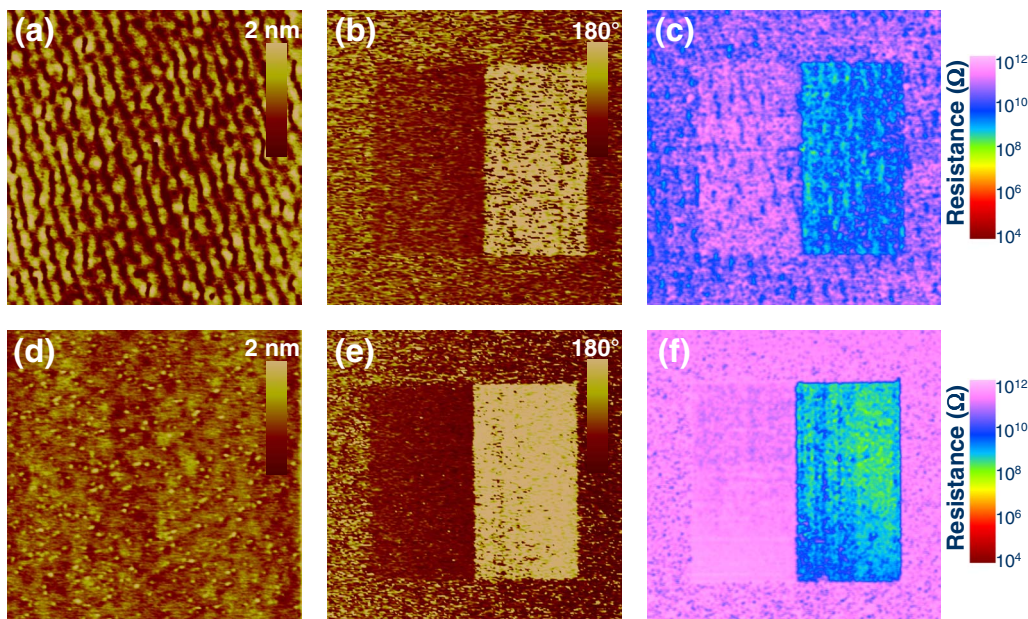


FIG. 2. (Color online) Ferroelectric and TER properties of PTO ultrathin films probed by PFM and CTAFM, respectively. $12 \times 12 \mu\text{m}^2$ (a) topography, (b) out-of-plane PFM phase images and (c) CTAFM resistance mapping of two written ferroelectric stripes ($4 \times 8 \mu\text{m}^2$) for PTO_{4ML}. $12 \times 12 \mu\text{m}^2$ (d) topography, (e) out-of-plane PFM phase images and (f) CTAFM resistance mapping of two written ferroelectric stripes ($4 \times 8 \mu\text{m}^2$) for PTO_{9ML}. The TER reaches 4,000% and 50 000% for PTO_{4ML} and PTO_{9ML}, respectively.

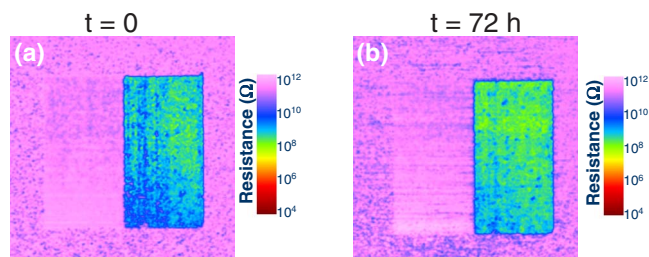


FIG. 3. (Color online) $12 \times 12 \mu\text{m}^2$ CTA FM resistance mapping of two written ferroelectric stripes ($4 \times 8 \mu\text{m}^2$) for $\text{PTO}_{9\text{ML}}$ observed (a) just after poling, (b) on the same area after 72 h.

the screening length of SRO (and LSMO) is larger than the tip one. Consequently, if one considers a purely electrostatic model, the barrier height will be lower when the ferroelectric polarization points toward SRO than when it points toward the tip.¹¹

Moreover, to verify that the OPP is directly correlated with the ferroelectricity of the ultrathin films, and not to injected charges during poling, a TER analysis of the poled region was performed 72 h after writing the ferroelectric pattern on the $\text{PTO}_{9\text{ML}}$ film (Fig. 3). Indeed, combining PFM and electrostatic force microscopy, 40 h were required for the residual surface charges to dissipate in 80 nm thick PZT thin films.¹⁸ PTO ultrathin films being structurally close, we took that time scale as a good estimate. The shape of the written domains and the value of the TER effect are roughly constant over this time scale.

In conclusion, epitaxial ultrathin PTO films were grown by PLD. Their ferroelectricity was demonstrated using PFM. PFM reveals a net out-of-plane phase contrast between domains polarized up and down. A giant TER effect reaching 50 000% for the 3.6 nm PTO barrier was measured combining PFM and CTA FM. This effect is stable in time at least up to 72 h. Our results demonstrate that the giant TER effect is not restricted to BaTiO_3 barriers but should be observable in all ferroelectrics. Challenges for the future are now the optimization of the barrier and electrode materials to achieve the largest effects, the fabrication of solid-state FTJs (i.e., with a

top electrode), and the study of the high-frequency dynamics of the TER effect.

The authors thank Javier Villegas for scientific discussions. This work was supported by French RTRA Triangle de la Physique, EU STRP Macomufi, French C-Nano Île de France, French ANR Oxitronics, French ANR Alicante, and French PRES UniverSud.

¹J. F. Scott, *Science* **315**, 954 (2007).

²M. Dawber, K. M. Rabe, and J. F. Scott, *Rev. Mod. Phys.* **77**, 1083 (2005).

³L. Esaki, R. B. Laibowitz, and P. J. Stiles, *IBM Tech. Discl. Bull.* **13**, 2161 (1971).

⁴L. Despont, C. Koitzsch, F. Clerc, M. G. Garnier, P. Aebi, C. Lichtensteiger, J.-M. Triscone, F. J. Garcia de Abajo, E. Bousquet, and Ph. Ghosez, *Phys. Rev. B* **73**, 094110 (2006).

⁵D. D. Fong, G. B. Stephenson, S. K. Streiffer, J. A. Eastman, O. Auciello, P. H. Fuoss, and C. Thompson, *Science* **304**, 1650 (2004).

⁶H. Béa, S. Fusil, K. Bouzehouane, M. Bibes, M. Sirena, G. Herranz, E. Jacquet, J.-P. Contour, and A. Barthélémy, *Jpn. J. Appl. Phys., Part 2* **45**, L187 (2006).

⁷V. Garcia, S. Fusil, K. Bouzehouane, S. Enouz-Vedrenne, N. D. Mathur, A. Barthélémy, and M. Bibes, *Nature (London)* **460**, 81 (2009).

⁸J. Rodriguez Contreras, H. Kohlstedt, U. Roppe, R. Waser, C. Buchal, and N. A. Pertsev, *Appl. Phys. Lett.* **83**, 4595 (2003).

⁹E. Y. Tsymlal and H. Kohlstedt, *Science* **313**, 181 (2006).

¹⁰H. Kohlstedt, N. A. Pertsev, J. Rodriguez Contreras, and R. Waser, *Phys. Rev. B* **72**, 125341 (2005).

¹¹M. Y. Zhuravlev, R. F. Sabirianov, S. S. Jaswal, and E. Y. Tsymlal, *Phys. Rev. Lett.* **94**, 246802 (2005); **102**, 169901 (2009).

¹²J. P. Velev, C.-G. Duan, J. D. Burton, A. Smogunov, M. K. Niranjan, E. Tosatti, S. S. Jaswal, and E. Y. Tsymlal, *Nano Lett.* **9**, 427 (2009).

¹³A. Gruverman, D. Wu, H. Lu, Y. Wang, H. W. Jang, C. M. Folkman, M. Y. Zhuravlev, D. Felker, M. Rzchowski, C.-B. Eom, and E. Y. Tsymlal, *Nano Lett.* **9**, 3539 (2009).

¹⁴G. Koster, B. L. Kropman, G. J. H. M. Rijnders, D. H. A. Blank, and H. Rogalla, *Appl. Phys. Lett.* **73**, 2920 (1998).

¹⁵G. J. H. M. Rijnders, G. Koster, D. H. A. Blank, and H. Rogalla, *Appl. Phys. Lett.* **70**, 1888 (1997).

¹⁶C. Lichtensteiger, M. Dawber, N. Stucki, J.-M. Triscone, J. Hoffman, J.-B. Yau, C. H. Ahn, L. Despont, and P. Aebi, *Appl. Phys. Lett.* **90**, 052907 (2007).

¹⁷*Nanoscale Characterisation of Ferroelectric Materials, Scanning Probe Microscopy Approach*, edited by M. Alexe and A. Gruverman (Springer, Berlin, 2004).

¹⁸T. Tybell, C. H. Ahn, and J.-M. Triscone, *Appl. Phys. Lett.* **75**, 856 (1999).